

# IEICE Proceeding Series

Bifurcation Structure of Augmented Lorenz Equations and  
Synchronizability of Coupled Augmented Lorenz Oscillators

Koki Yoshimito, Kenichiro Cho, Yuichiro Morita, Takaya Miyano

Vol. 1 pp. 789-792

Publication Date: 2014/03/17

Online ISSN: 2188-5079

Downloaded from [www.proceeding.ieice.org](http://www.proceeding.ieice.org)



# Bifurcation Structure of Augmented Lorenz Equations and Synchronizability of Coupled Augmented Lorenz Oscillators

Koki Yoshimito, Kenichiro Cho, Yuichiro Morita and Takaya Miyano

Graduate School of Science and Engineering, Ritsumeikan University  
1-1-1 Noji-Higashi, Kusatsu, Shiga, 525-8577 Japan  
Email: tmiyano@se.ritsumei.ac.jp

**Abstract**—The bifurcation structure of the augmented Lorenz equations as a starlike network of Lorenz subsystems is investigated as a function of the reduced Rayleigh number and the number of Lorenz subsystems by performing numerical simulations. Estimated bifurcation diagrams are discussed in relation to chaotic synchronization of directly coupled augmented oscillators with parameter mismatch.

## 1. Introduction

Motivated by the chaotic waterwheel whose rotational motion is governed by the Lorenz equations [1]–[3], we recently developed a chaotic gas turbine that randomly reverses its direction of rotation [4]–[7] simulating the motion of the convective roll in turbulent Rayleigh-Bénard convection at high Rayleigh numbers exceeding  $10^6$  [8]–[10]. Our gas turbine is a planar type that is often used for designing micro gas turbine engines based on micro-electro-mechanical systems [11, 12]. However, our machine is driven by the aerodynamic drag generated on its turbine blades staying within a limited space (referred to as the working range) around the central axis of the turbine, unlike existing gas turbines whose rotational motions are driven by aerodynamic lift. As a result, the equations of motion of our turbine are represented as a particular system of nonlinear ordinary differential equations. That is, the nondimensionalized expressions for the equations of motion are represented as a starlike network of infinitely many Lorenz subsystems sharing the dimensionless angular velocity as the central node. We refer to the nondimensionalized equations with the number of Lorenz subsystems truncated at a fine number of  $N$  as augmented Lorenz equations.

The augmented Lorenz equations are dependent on three dimensionless parameters defined in terms of the mechanical parameters of the turbine. These parameters entirely determine the dynamical properties of the augmented Lorenz equations. Two of these dimensionless parameters are equivalent to the Prandtl number and the reduced Rayleigh number for Rayleigh-Bénard convection [4, 7]. The applicability of the augmented Lorenz model is not restricted to the chaotic gas tur-

bine when the model is viewed as a general dynamical model. Then, the three dimensionless parameters specifying the augmented Lorenz model are no longer bound by the mechanical structure of the turbine and can instead be set to arbitrary real numbers convenient for the application in hand. For instance, coupled nonlinear oscillators governed by the augmented Lorenz equations are applicable to chaos-based communications using chaotic masking [13, 14]. However, the bifurcation structure of the augmented Lorenz model is indispensable for developing such applications. Although the augmented Lorenz model inherits the dynamical nature of the Lorenz model whose bifurcation structure has been well investigated [15, 16], much is unknown about its bifurcation structure.

In this paper, we examine the bifurcation structure of the augmented Lorenz model using numerical simulations, focusing on its dependence on the reduced Rayleigh number and the number of Lorenz subsystems. The working range and the Prandtl number are fixed at the values that give rise to chaos for the chaotic gas turbine. We also assess the chaotic synchronizability of directly coupled oscillators governed by the augmented Lorenz equations as a function of parameter mismatch in the equations. Estimated bifurcation diagrams are discussed in relation to the chaotic synchronizability of the coupled oscillators. In real-world applications, coupled oscillators inevitably have parameter mismatch in the dynamics governing the oscillators. The degree of synchronizability of the coupled oscillators as a function of parameter mismatch is important information in the development of real-world applications.

## 2. Theory

In this section, we give a brief summary for the augmented Lorenz model. Details will be given elsewhere [7]. The augmented Lorenz equations simulate the physical aspects of Rayleigh-Bénard convection of fluids heated from below and cooled from above in much the same way as the Lorenz model. That is, buoyancy, viscous drag and thermal dissipation are embedded into the Prandtl number and the reduced Rayleigh

number. The augmented Lorenz equations as a general dynamical model are given as

$$\frac{dX}{d\tau} = \sigma [\text{tr}((\mathbf{n}^{-1})^2 \mathbf{Y}) - X] , \quad (1)$$

$$\frac{d\mathbf{Y}}{d\tau} = \mathbf{R}X - \mathbf{n}\mathbf{Z}X - \mathbf{Y} , \quad (2)$$

$$\frac{d\mathbf{Z}}{d\tau} = \mathbf{n}\mathbf{Y}X - \mathbf{Z} , \quad (3)$$

$$\mathbf{R} = R_0 \mathbf{n}^2 \Phi \mathbf{W} ,$$

where  $X$  is a dimensionless scalar variable,  $\mathbf{Y}$  and  $\mathbf{Z}$  are dimensionless  $N \times N$  diagonal matrices whose diagonal components  $Y_n$  and  $Z_n$  with  $n$  running from 1 to  $N$  represent dimensionless scalar variables, respectively,  $\tau$  is dimensionless time,  $\text{tr}(\cdot)$  denotes the diagonal sum of a matrix,  $\sigma$  and  $R_0$  are dimensionless scalar parameters. Dimensionless matrix  $\mathbf{R}$  is defined using  $\mathbf{n} = \text{diag}(1, 2, \dots, N)$ ,  $\mathbf{W} = \text{diag}(\sin \phi, \sin 2\phi, \dots, \sin N\phi)$  and  $\Phi = \text{diag}\left(\phi - \frac{1}{2} \sin 2\phi \cdots \frac{1}{n-1} \sin(n-1)\phi - \frac{1}{n+1} \sin(n+1)\phi \cdots \frac{1}{N-1} \sin(N-1)\phi - \frac{1}{N+1} \sin(N+1)\phi\right)$ , where  $\phi$  is the working range.

When  $N = 1$ , Eqs. (1)–(3) are exactly equivalent to the Lorenz equations with a geometric parameter of unity. In this sense,  $\sigma$  and  $R_0$  correspond to the Prandtl number and the reduced Rayleigh number, respectively. Equations (1)–(3) can be viewed as a starlike network of  $N$  Lorenz subsystems sharing  $X$  as the central node.

Nonlinear oscillators governed by the augmented Lorenz equations can be coupled via the direct coupling of  $X$  or  $\mathbf{Y}$ . Let us consider a drive-response system consisting of two augmented Lorenz oscillators. When the drive system is subject to Eqs. (1)–(3), the response system is subject to

$$X' = X , \quad (4)$$

$$\dot{\mathbf{Y}}' = \mathbf{R}'X' - \mathbf{n}\mathbf{Z}'X' - \mathbf{Y}' , \quad (5)$$

$$\dot{\mathbf{Z}}' = \mathbf{n}\mathbf{Y}'X' - \mathbf{Z}' , \quad (6)$$

for the direct coupling of  $X$  or

$$\dot{X}' = \sigma' [\text{tr}((\mathbf{n}^{-1})^2 \mathbf{Y}') - X'] , \quad (7)$$

$$\dot{\mathbf{Y}}' = \mathbf{Y}' , \quad (8)$$

$$\dot{\mathbf{Z}}' = \mathbf{n}\mathbf{Y}'X' - \mathbf{Z}' , \quad (9)$$

for the direct coupling of  $\mathbf{Y}$ , where  $X'$ ,  $\mathbf{Y}'$  and  $\mathbf{Z}'$  denote the variables for the response system,  $\mathbf{R}'$  includes the reduced Rayleigh number  $R'_0$  and  $\sigma'$  is the Prandtl number, specifying the response system, respectively.

### 3. Numerical Analysis

In this study, the working range  $\phi$  and the Prandtl number  $\sigma$  are fixed at  $\phi = 0.36$  [rad] and  $\sigma = 28.3$ , respectively. These parameter settings generate chaotic

motion for the chaotic gas turbine [4, 6, 7]. Bifurcation diagrams of the augmented Lorenz model were estimated as functions of  $R_0$  and  $N$  by numerically integrating Eqs. (1)–(3) using the fourth-order Runge-Kutta method with a dimensionless time width of  $4 \times 10^{-5}$  for  $0 \leq R_0 \leq 3500$  and  $1 < N \leq 1000$ . The minimum difference between adjacent values of  $R_0$  was set to  $\Delta R_0 = 1$ . The initial value of  $X$  was given as  $X(0) = 0$  and those of  $Y_n$  and  $Z_n$  were given as Gaussian random numbers with mean 0 and variance 1. The initial 250 000 solutions were discarded to eliminate the initial transient solutions depending on the initial conditions.

Figure 1 shows estimated bifurcation diagrams as functions of  $R_0$  at  $N = 100$ . The estimated diagrams correspond to the cross-sectional plots for  $-0.01 \leq Y_{10} \leq 0.01$  if  $N \geq 10$  and those for  $-0.01 \leq Y_{N-1} \leq 0.01$  otherwise. The general features of the bifurcation diagrams are qualitatively similar to that of the Lorenz model, despite some minor differences. The threshold of  $R_0$  for the onset of chaos was found to shift from  $\sim 500$  to  $\sim 1200$  as  $N$  increases from 5 to 6 and approach  $\sim 1500$  at  $N = 100$ . A window in which chaotic oscillations are superseded by nonchaotic oscillations appears between  $\sim 1600$  and  $\sim 1800$  when  $N$  exceeds 350. It can be seen that chaos is well developed at  $R_0 \geq 2000$ .

We next measured the synchronization error between two augmented Lorenz oscillators coupled via the direct coupling of  $X$  under parameter mismatch in  $R_0$ . The drive oscillator is governed by Eqs. (1)–(3) and the response oscillator by Eqs. (4)–(6). Comparing Eqs. (4)–(6) with Eqs. (7)–(9), the synchronization error due to the direct coupling of  $X$  is found to be induced by the parameter mismatch in  $R_0$ , not by that in  $\sigma$ . The rate of parameter mismatch in  $R_0$  is defined as  $r = (R'_0 - R_0)/R_0$ . We assume that the coupled oscillators with  $N = 100$  are a typical system in the application of the augmented Lorenz model to chaotic synchronization. In this case, the chaotic oscillation is well developed around  $R_0 = 3000$  as shown in Fig. 1.

For  $r$  increasing from  $-0.1$  to  $0.1$  around  $R_0 = 3000$  with an increment width of 0.01, Eqs. (1)–(3) and Eqs. (4)–(6) with  $N = 100$  were numerically integrated using the fourth-order Runge-Kutta method with a dimensionless time width of  $4 \times 10^{-5}$ . The initial 450 000 solutions were discarded to eliminate the initial transient part of the synchronization process. Then, the synchronization error was estimated for  $T = 50$  000 solutions of  $Z_n$  and  $Z'_n$  at each  $r$ . The synchronization error  $E(r)$  as a function of  $r$  is defined as

$$E(r) = \frac{1}{T} \sum_{t=1}^T \sqrt{\frac{1}{N} \sum_{n=1}^N [Z'_n(t, r) - Z_n(t)]^2} . \quad (10)$$

Results are shown in Fig. 2. The synchronization error

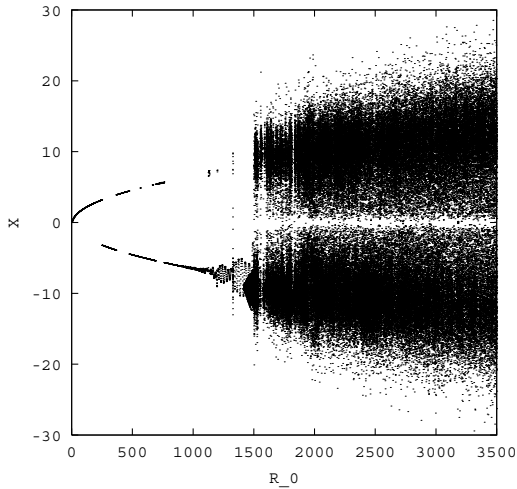


Figure 1: Bifurcation diagram as function of  $R_0$  at  $N = 100$  ( $\sigma = 28.3$ ).

at  $r = 0$ , i.e., with no parameter mismatch, was estimated to be  $E(0) \approx 0.006$ . The increase in  $E(r)$  with increasing parameter mismatch is linear with respect to  $|r|$  and symmetrical around  $r = 0$ .

#### 4. Discussion

The general features of the bifurcation structure of the augmented Lorenz model are qualitatively similar to that of the Lorenz model. This suggests that the augmented Lorenz model inherits the dynamical nature of the Lorenz model. In fact, chaotic synchronization is also achieved via the direct coupling of  $X$  for the coupled augmented Lorenz oscillators in much the same way as coupled Lorenz oscillators.

In applications of the augmented Lorenz model such as chaos-based communications based on chaotic masking, large-scale oscillators would be required to generate chaos with a sufficient degree of complexity. For such demands, augmented Lorenz oscillators with  $N = 100$  would suffice. In real-world applications, parameter mismatch between the drive system and response system is often inevitable. Our results indicate that the rate of increment in the synchronization error is approximately 36 times as large as the synchronization error at no parameter mismatch per 1 % of parameter mismatch. These estimates will be useful for designing the tolerance of a secure communication system based on chaotic masking to parameter mismatch as well as for determining the minimal difference between adjacent encryption-decryption keys in the  $R_0$ -key space.

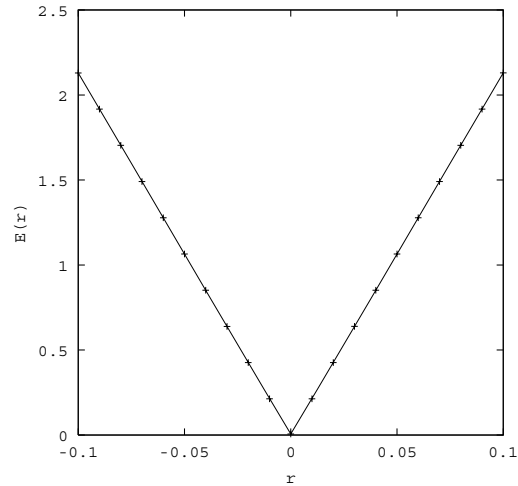


Figure 2: Synchronization error  $E(r)$  as function of rate of parameter mismatch  $r$ .  $R_0 = 3000$  and  $N = 100$  ( $\sigma = 28.3$ ).

#### 5. Conclusions

We examined the bifurcation structure of the augmented Lorenz model as a function of the reduced Rayleigh number  $R_0$  and the number of Lorenz subsystems  $N$ . The bifurcation structure was found to be qualitatively similar to that of the Lorenz model. The synchronization error between two augmented Lorenz oscillators with  $N = 100$  coupled via the direct coupling of  $X$  was estimated as a function of parameter mismatch in  $R_0$  around  $R_0 = 3000$  and was found to increase linearly with increasing rate of parameter mismatch. The application of the augmented Lorenz model to real-world problems is an open question to be investigated in future studies.

#### Acknowledgments

We thank Professor Toshiyuki Toriyama for helpful advice and stimulating discussion. This study was supported by JSPS Grant-in-Aid for Scientific Research (C) No. 22500214.

#### References

- [1] S. H. Strogatz, *Nonlinear Dynamics and Chaos* (Addison-Wesley, Massachusetts, 1994) Chapter 9.
- [2] M. Kolar and G. Gumbs, "Theory for the experimental observation of chaos in a rotating water-wheel," *Phys. Rev. A*, vol.45, pp.626–637, 1992.
- [3] E. N. Lorenz, "Deterministic non-periodic flow," *J. Atmos. Sci.*, vol.20, pp.130–141, 1963.

- [4] K. Cho, Y. Okada, J. Tatsutani, T. Toriyama, T. Miyano, "Chaotic Gas Turbine Simulating the Motion of Convective Heat Flow," *Proc. 2011 Int. Symp. Nonlin. Theor. Appl. (NOLTA2011)*, pp.13-16, 2011.
- [5] K. Cho, J. Tatsutani, T. Miyano, "Chaotic Synchronization of Augmented Lorenz Systems," *Proc. 2011 Int. Symp. Nonlin. Theor. Appl. (NOLTA2011)*, pp.476-479, 2011.
- [6] T. Miyano, K. Cho, Y. Okada, J. Tatsutani, T. Toriyama, "Augmented Lorenz Equations as Physical Model for Chaotic Gas Turbine," *Procedia IUTAM*, in print.
- [7] K. Cho, T. Miyano, T. Toriyama, submitted.
- [8] K. R. Sreenivasan, A. Bershadskii and J. J. Niemela, "Mean Wind and its Reversal in Thermal Convection," *Phys. Rev. E*, vol.65, 056306, 2002.
- [9] F. Fontenele Araujo, S. Grossmann and D. Lohse, "Wind Reversals in Turbulent Rayleigh-Bénard Convection," *Phys. Rev. Lett.*, vol.95, 084502, 2005.
- [10] G. Ahlers, S. Grossmann and D. Lohse, "Heat transfer and large scale dynamics in turbulent Rayleigh-Benard convection," *Rev. Mod. Phys.*, vol.81, pp.503–537, 2009.
- [11] A. H. Epstein and S. D. Senturia, "Macro Power from Micro Machinery," *Science*, vol.276, p.1211, 1997.
- [12] A. H. Epstein, "Millimeter-scale, Micro-Electro-Mechanical Systems Gas Turbine Engines," *ASME J. Eng. Gas Turbine Power*, vol.126, pp.205–226, 2004.
- [13] K. M. Cuomo and A. V. Oppenheim, "Circuit Implementation of Synchronized Chaos with Applications to Communications," *Phys. Rev. Lett.*, vol.71, no.1, pp.65–68, 1993.
- [14] K. M. Cuomo, A. V. Oppenheim and S. H. Strogatz, "Synchronization of Lorenz-based chaotic circuits with applications to communications," *IEEE Trans. Circuits Syst. II*, vol.40, pp.626–633, 1993.
- [15] R. Barrio and S. Serrano, "A three-parametric study of the Lorenz model," *Physica D*, vol.229, pp.43–51, 2007.
- [16] R. Barrio and S. Serrano, "Bounds for the chaotic region in the Lorenz model," *Physica D*, vol.238, pp.1615–1624, 2009.